

Monitoring Kinetic Processes in Polymer Solutions with Time Dependent Static Light Scattering (TDSLS)

Wayne F. Reed

Physics Dept.

Tulane University

New Orleans, La. 70118, USA

SUMMARY: An overview of recent developments in TDSLS and auxiliary techniques is given. This includes background theory, and examples of results and applications for online monitoring of polymerization reactions, kinetics and structural determinations from degrading polymers, aggregation, and dissolution of dry polymer powders. Also, automatic dilution techniques allow for continuous characterization of the equilibrium states of multi-component solutions. Illustrations are given for the case where the change in polyelectrolyte dimensions, interactions and hydrodynamics can be probed.

Introduction

Light scattering techniques have traditionally been used for characterizing the equilibrium properties of polymer solutions. Since changes in light scattering intensity and angular distribution can easily be monitored on the time scale of many kinetic processes, TDSLS is a useful tool for characterizing such phenomena. These latter include the polymerization process itself, polymer degradation, microgel formation, aggregation, and dry polymer dissolution. Additionally, TDSLS lends itself naturally to automated forms of equilibrium characterization. There has been a recent increase in activity in TDSLS and related techniques, including instrumentation.^{1,2,3} Formation of complexes and aggregation in both bio- and synthetic polymer solutions has been reported,^{4,5,6,7,8,9,10,11} as well as phase separation phenomena,^{12,13,14,15,16,17} crystallization,^{18,19} and degradation.²⁰

Use of the Zimm approximation

The most widely used light scattering approximation for polymers, due to Zimm,²¹ is normally expressed as the excess Rayleigh scattering $I(q, c_p)$, which is total solution scattering minus solvent scattering background, and is a function of polymer concentration c_p and scattering vector q . In TDSLS, the scattering is also a function of time, so that it can be written in terms of q , c_p and t , $I(q, c_p, t)$. Zimm's equation becomes:

$$\frac{Kc_p}{I(q, c_p, t)} = \frac{1}{MP(q)} + 2A_2c_p + [3A_3Q(q) - 4A_2^2MP(q)(1 - P(q))]c_p^2 \quad (1)$$

where it is understood that all parameters K , c_p , M , $P(q)$, etc. are potentially functions of t . This equation forms the basis of the Zimm plot, which, at low concentrations and for $q^2 \langle S^2 \rangle \ll 1$ can be written, for a polydisperse polymer population as

$$\frac{Kc_p}{I(q, c_p)} = \frac{1}{M_w} \left(1 + \frac{q^2 \langle S^2 \rangle_z}{3} \right) + 2A_2c_p \quad (2)$$

which directly permits determination of weight averaged molecular mass M_w , second virial coefficient A_2 , and the z -averaged mean square radius of gyration $\langle S^2 \rangle_z$. K is an optical constant, given for vertically polarized incident light by

$$K = \frac{4\pi^2 n^2 (dn/dc_p)^2}{N_A \lambda^4} \quad (3)$$

where n is the solvent refractive index, λ is the laser vacuum wavelength, dn/dc_p is the differential refractive index for the polymer/solvent, and $q = (4\pi n/\lambda) \sin(\theta/2)$, where θ is the scattering angle.

This equation is based on the Rayleigh-Debye approximation, in which it is assumed that the phase shift accrued by a scattered wave traversing the scattering particle itself is due purely to the geometrical path length covered; i.e the difference in index of refraction between the scatterer and the solvent adds negligibly to the phase shift. For polymers, this approximation is usually quite good, since the polymer is a thread-like entity of scatterers immersed in a solvent. When the scatterers become dense, or solid, such as can occur in aggregation and crystallization phenomena, this approximation quickly breaks down, and the scattering problem requires a full solution of Maxwell's equations within and without the scatterer, and matched boundary conditions. This latter approach is often termed 'Mie scattering'.^{22,23}

Instrumentation and methods

The detection portion of all the monitoring experiments involves some combination of the following instruments: a multi-angle TDSLS detector, a viscometer, a refractometer (RI), and an ultra-violet absorption detector (UV). TDSLS detectors used have included both home-built units, previously described in detail,²⁴ and a Wyatt Technologies Dawn-

F. In fact, this same detector train is also used for traditional multi-detector Gel Permeation Chromatography (GPC).^{25,26}

The significant differences between the monitoring experiments involve sample conditioning and handling. The main requirement for monitoring is to produce a continuous stream of dilute sample, so that absolute light scattering, and viscosities approaching intrinsic viscosity, can be measured. In some instances the polymer solution in the reactor is so concentrated it must be continuously diluted. In others there are macroscopic particles in the polymer solution that need to be filtered (e.g. dissolution of dried polymers), whereas in other cases temperature conditions might be desired that are difficult to create and maintain in the detectors (e.g. high and low temperature degradation reactions). Means of sample conditioning have been developed for each scenario, although it is a continuing challenge to find means of handling the sampling aspect for increasingly complex systems.

Online monitoring of polymerization reactions

The ability to perform automatic, continuous online monitoring of polymerization reactions (ACOMP) is of interest in three main areas: At the fundamental level, polymer chemists can immediately observe the effects of different synthetic strategies, monomers, initiators, and other factors, and how they influence kinetics and polymer properties. This should prove to be a significant advance for new material discovery. Industrial scientists can use monitoring as a tool for pilot plant optimization of industrial processes. One of the ultimate goals of ACOMP is to apply it to full scale industrial reactors, integrated into a feedback loop that can control reactions. This promises to have a great economic and ecological impact on how large industrial polymer producers operate. Monitoring kinetics of polymerization reactions requires that measurements be made either periodically or continuously on a reacting solution. One of the first works is due to Flory²⁷, who manually withdrew aliquots from a glycol/dibasic acid polyesterification reaction every ten minutes and performed a KOH titration to estimate M_w and rate constants. Bresler et al.²⁸ made periodic ESR measurements to follow radical concentrations in homogeneous polymerization reactions of methyl methacrylate and vinyl acetate. Shen and Tian used ESR simultaneously to measure radical concentration and monomer conversion in methyl methacrylate polymerization at intervals a few

minutes apart.²⁹ Ballard and van Lienden³⁰ used dilatometry to estimate initial polymerization rates of vinyl monomers by metal compounds.

Real-time monitoring of polymerization is a more recent development. Near-IR^{31,32,33,34,35,36,37,38,39,40} (near IR), ultra-violet (uv)^{41,42} and fluorescence⁴³ monitoring are proving particularly useful for measurements of monomer conversion and process completion. Fluorescence techniques are also being used for monitoring curing reactions of epoxies.^{44,45} IR studies have also been used to estimate copolymer composition and rheological properties⁴⁶, whereas direct rheological techniques are being used to estimate molecular weight online.^{47,48,49} Monitoring post-pulse processes in laser induced polymerization has also been reported.⁵⁰ The author was previously involved in surfactant vesicle laser-induced polymerization, in which laser flash photolysis was used to follow monomer conversion rates.^{51,52}

ACOMP has recently been introduced.⁵³ It allows M_w , monomer conversion f , intrinsic viscosity $[\eta]$, and certain measures of polydispersity to be followed in near real-time, without the use of chromatographic columns. The method requires that a continuous stream of dilute polymer/monomer solution pass through a train of detectors, normally comprising TDSLS, refractometer (RI), ultra-violet absorbance (UV), and viscosity detectors. For chain growth reactions, the UV detector has been used to follow the disappearance of double bonds in many types of polymerization reactions, which allows both the conversion to be monitored, and M_w to be computed, since only the polymer concentration figures into the computation of M_w . In contrast, for step-growth reactions both monomer and polymer concentrations figure into the computation of M_w , so that no concentration detectors are needed.

The dilute stream is produced by continuously withdrawing a small amount of reactor liquid (typically 50 $\mu\text{L}/\text{min}$) and mixing it with a much larger volume of pure solvent (typically 1.95 mL/min). This has been achieved both with low pressure mixing, involving a programmable gradient mixer in conjunction with a single isocratic pump, and a high pressure scheme using two isocratic pumps and a micro-mixing chamber.

Raw data from a typical polymerization reaction, that of acrylamide,⁵⁴ is shown in figure 1. The stabilization of detectors with pure solvent for the first 500 seconds is seen, followed by stabilization with a stream consisting of 4% reactor liquid and 96% water

from a reservoir (total monomer concentration is 0.0014 g/cm^3). At 1600s a persulfate initiator was added and the polymerization can be seen by an increase in light scattering and viscosity signals, and a decrease in the UV, as the monomer double bond absorption is lost when the monomer is incorporated into a polymer chain.

Figure 1. Raw data for an acrylamide polymerization reaction at $T=70^\circ\text{C}$ (adapted from Giz et al., ref. 54)

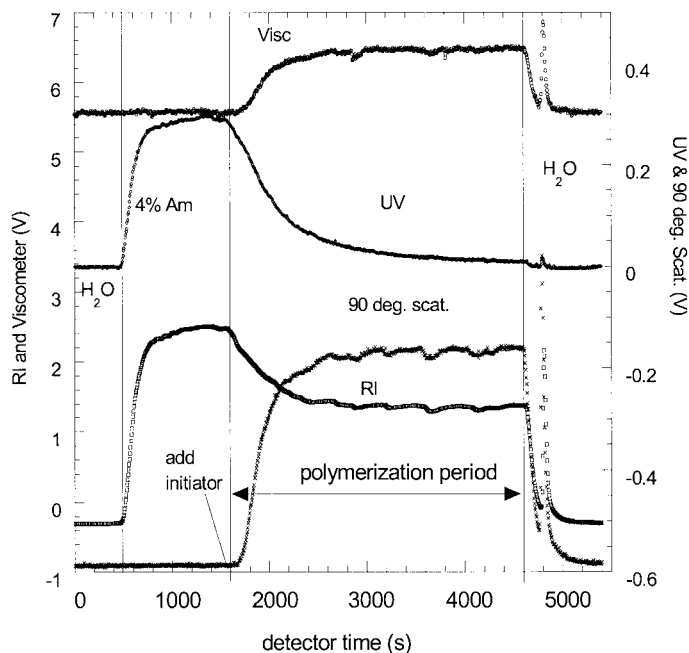
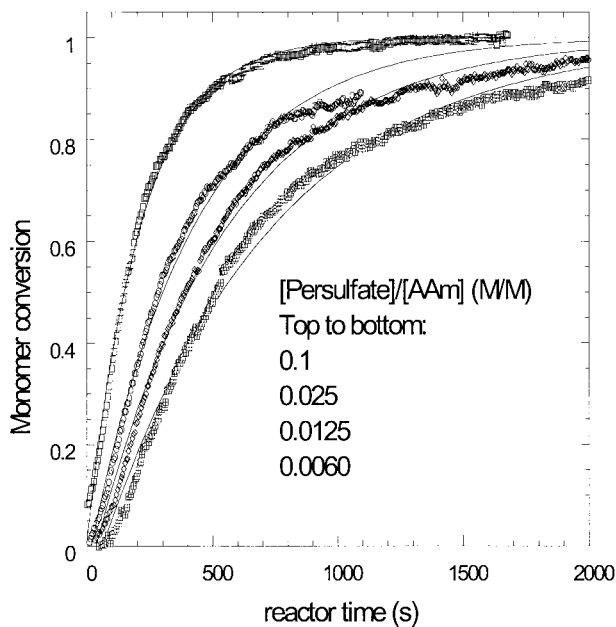


Figure 2 shows conversion curves for acrylamide polymerization reactions. The conversion is first order (exponential) when a high concentration of initiator is used, which is expected for ideal free radical polymerization.⁵⁵

Figure 2. Monomer conversion vs. time for the data of figure 1.
(Adapted from Giz et al., ref. 54)



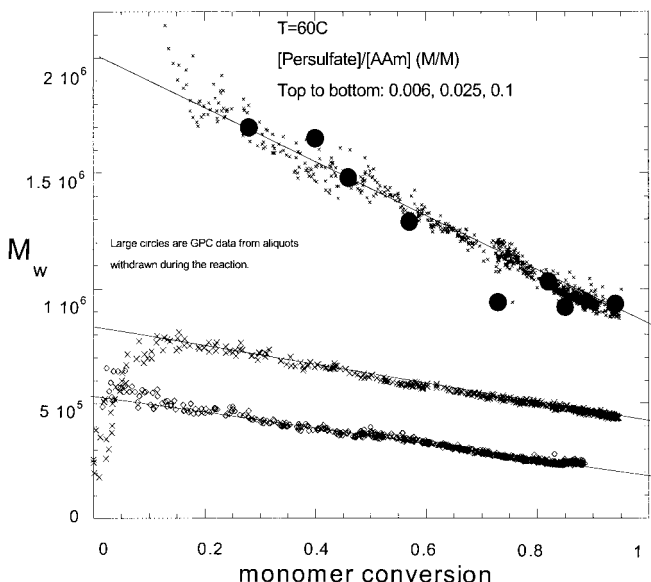
At lower initiator concentration, deviations from first order behavior are apparent at early and late conversion. This has been interpreted in terms of initial competition for radicals from impurities, and cage effects.^{54,56,57} M_w vs. conversion for typical reactions is shown in figure 3. Over the majority of conversion the decrease of M_w closely follows the predictions of ideal free radical polymerization, namely⁵⁴

$$M_w(f) = M_w(0)(1 - f/2) \quad (4)$$

The deviation from this occurs at early conversion.

Figure 3. M_w vs. conversion for various acrylamide polymerization reactions.

The linear regime that sets in at early conversion reflects ideal free radical polymerization. (Adapted from Giz et al., ref. 54)



Because ACOMP uses no chromatographic columns or other separation techniques, to which it owes its near real-time advantages, it is interesting to see how much information it can provide on the evolution of polydispersity during polymerization reactions. This area was recently considered, and it was found there are at least three immediate approaches.⁵⁸ The first is applicable when the polymers are large enough to give a measurable angular dependence for scattered light, which usually requires $\langle S^2 \rangle^{1/2}$ to be ten nanometers or higher. The slope of $Kc/I(q,c)$ is

$$\frac{d(Kc_p / I(q))}{dq^2} = \frac{\langle S^2 \rangle_z}{3M_w} = A \frac{\langle M^\beta \rangle_z}{M_w} \quad (5)$$

where β is the exponent linking $\langle S^2 \rangle$ to M ; $\langle S^2 \rangle = 3AM^\beta$. For the case of ideal coils $\beta=1$, so that the slope is directly proportional to M_z/M_w . For coils with excluded volume $\beta \sim 1.2$, and so the slope will be proportional to a quantity slightly higher than M_z/M_w .

This measure of polydispersity is automatically collected during ACOMP, as long as the polymers have a measurable $\langle S^2 \rangle^{1/2}$ (typically a minimum of 10nm).

A second means of monitoring the evolution of polydispersity is by combining the simultaneously measured viscosity and scattering data. It is then possible to obtain the quantity M_w/M_η , where M_η is the viscosity average mass, which often falls between M_n and M_w . In principle, the combination of viscosity and M_w data should also prove valuable for following branching during polymerization reactions, since M_w combined with $[\eta]$ yields the polymer's hydrodynamic volume. Light scattering and viscosity have frequently been used to determine branching.^{59,60,61}

For chain growth reactions where dead polymer chains are rapidly produced compared to the time needed for total monomer conversion, it is possible to compute the instantaneous weight average molecular weight, $M_{w,inst}$, according to:

$$M_{w,inst}(f) = M_w(f) + f \left. \frac{dM_w}{df} \right|_f \quad (6)$$

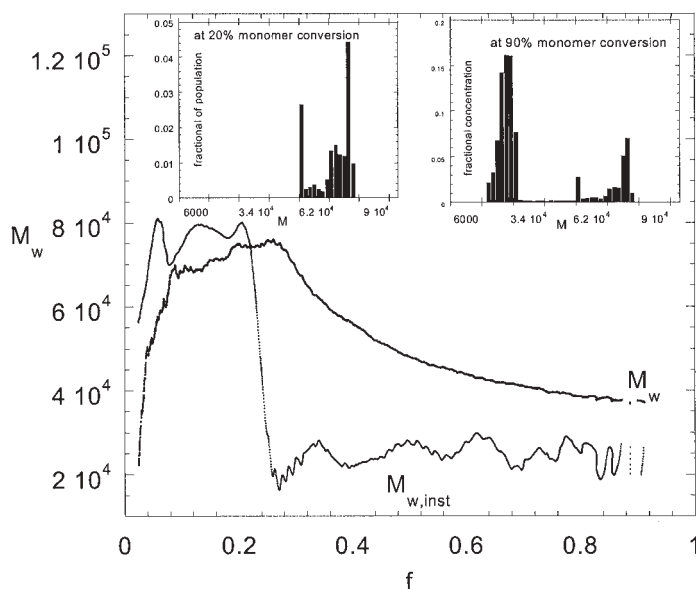
Figure 4 shows data for the polymerization of poly(vinyl pyrrolidone), or PVP,⁵³ and the computation of $M_{w,inst}$.⁵⁸ It was found that M_w stayed at a constant level throughout conversion, although no convincing explanation for this was found. In fig. 4 PVP polymerization occurred at a constant M_w , and then a boost of hydrogen peroxide initiator was given to the reactor at 20% conversion. The effect was to make the remaining monomer build to polymers of lower M_w for the remainder of the conversion. The cumulative M_w decreases smoothly, as shown, so it is not evident that a bimodal population is produced. $M_{w,inst}$, plotted on the same curve, however, clearly shows that $M_{w,inst}$ quickly plunges to a much lower value, as soon as initiator is injected.

The computation of $M_{w,inst}$ from the ACOMP data requires no model dependent assumptions. If one wishes to obtain absolute polydispersity indices, such as M_w/M_n or M_z/M_w , then model dependent assumptions must be made. For free radical polymerization, where termination is by disproportionation, the instantaneous values of $M_{z,inst}$, $M_{w,inst}$ and $M_{n,inst}$ stand in the ratio 3:2:1. For termination by recombination $M_w/M_n = 3:2$. Hence, knowing $M_{w,inst}$ allows computation of $M_{z,inst}$ and $M_{n,inst}$, as well as any other conceivable average resulting from ideal free radical polymerization. The

insets to figure 4 show histogram distributions of the polymer population at 20% and 90% monomer conversion, derived from $M_{w,inst}$.

ACOMP has also been used to follow step growth reactions,⁶² and for controlled radical polymerization (CRP).⁶³ CRP combines the advantages of narrow polydispersity and controllable chain architecture of living polymerization with the robust, economical nature of free radical polymerization. ACOMP has been adapted to continuous reactors,⁶⁴ and used to determine chain transfer constants.⁶⁵ Current and future applications will include copolymerization and inhomogeneous phase polymerization.

Figure 4. Cumulative M_w and $M_{w,inst}$ for a vinyl pyrrolidone polymerization reaction, and distribution histograms (Adapted from ref. 58)



Degradation of polymers

When polymers are degraded under the influence of agents such as acids, bases, enzymes, heat, and radiation, the light scattering intensity will drop. The physical problem is to find a quantitative expression linking the time course of light scattering to the kinetics

and mechanisms causing the degradation, and to the polymer structure; i.e. whether the polymer is singly or multiply stranded, branched, etc.

The first deductions about polymer structure made from periodic sampling during a degradation reaction were due to Thomas,⁶⁶ who used the quadratically increasing number of cleavages in time to deduce that DNA was double-stranded. Since then, a general formalism for computing the time and wave vector dependent scattering $I(q,t)$ has been presented,⁶⁷ and signatures for a variety of degradation mechanisms and polymer structures have been predicted and found experimentally.^{68,69,70,71,72}

Figure 5 (adapted from ref. 72) shows the UV degradation of polystyrene that has a small percentage of methyl vinyl ketone (MVK) links. The initial degradation rate increases proportionately with the percentage of MVK links. Degradation is by random cleavage of single polymer chains.

Figure 5. UV degradation of MVK substituted PS. Figure 6. PG degradation

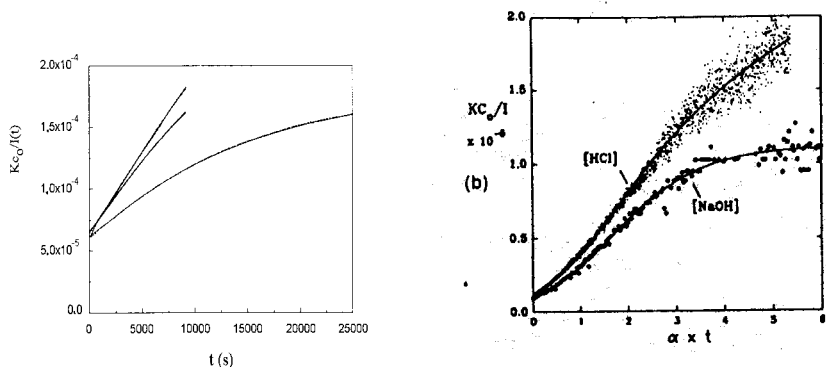


Figure 6 (adapted from ref. 71) shows the degradation of proteoglycan subunits (PG) under HCl and NaOH. The PG are composed of a protein backbone, to which short (2-20 kg/molc), sulfonated polysaccharide chains are covalently linked. The signature for NaOH indicates that degradation is via stripping of sidechains at the covalent link, whereas the signature for HCl shows that both sidechain stripping and random

degradation of the protein backbone are occurring. The expressions for the signatures allow degradation rates and fraction of material contained in the backbone and sidechains to be determined, as well as the degradation mechanism. Distinct signatures are calculated and found both for different types of degradation (e.g. endocytic and exocytic enzymatic cleavage, combinations of enzymes,⁷³ center-weighted scission, etc.), but also for different architectures; single and multiple strand chains and different types of branching. Hence, degradation studies can also be useful for determination of structure, such as branching, in addition to kinetics.

Dissolution of dry polymeric powders

The rate at which dry polymers dissolve in a solvent is an important characteristic in pharmaceutical, food, and general polymer sectors, and has been studied theoretically and experimentally.^{74,75,76} For possible uses of ACOMP where polymer is formed in the solid phase (e.g. fluidized bed), the dissolution time will be of critical importance in determining feasibility of ACOMP.

Michel and Reed⁷⁷ constructed a dissolution reactor by using a stirred beaker in a thermostated bath, and a peristaltic pump that filtered and circulated reactor liquid through the detector train. It was shown that the concentration of dissolved polymer $C_p(t)$, followed the expected third order dependence in time,⁷⁸

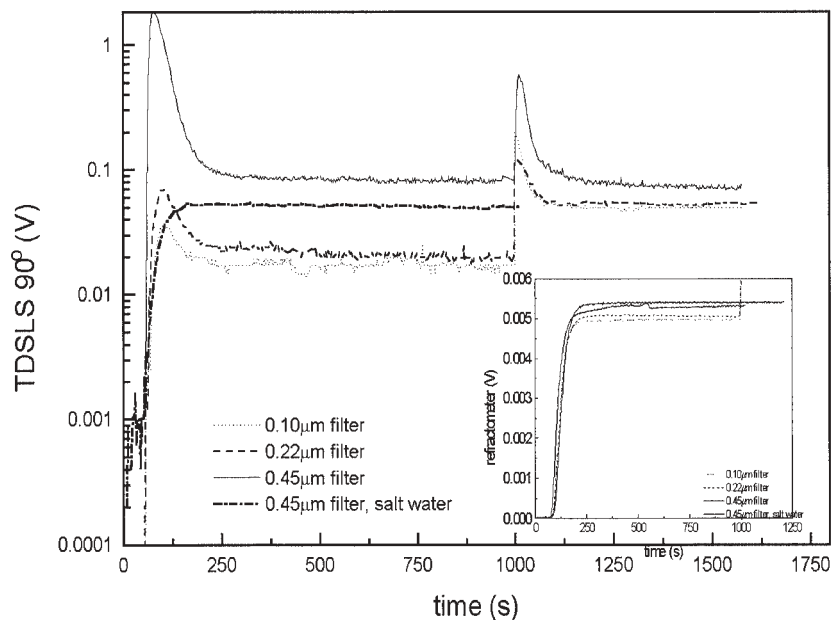
$$C_p(t) = C_o \left[1 - \left(1 - kt / R_o \right)^3 \right], \quad kt \leq R_o \quad (7)$$

and, was used to explore the effect of ionic strength on dissolution of polyelectrolytes.

Figure 7 shows dissolution data for sodium poly(styrene sulfonate) (PSS). The RI data in the inset show that there is no appreciable difference in dissolution rates whether the PSS is dissolved in pure water or salt water (0.1M NaCl), and is also independent of the pore size of the inline filtration membrane. The TDSLS data, however, depend significantly on whether pure water or salt water is used, and also on the size of the filter. In pure water there are initial spikes in the light scattering, which are so large that a logarithmic scale is used for the TDSLS voltage. The larger the pore size, the larger the effect. The spike is due to a small population of transient aggregates present as the polyelectrolyte dissolves in pure water. The aggregates eventually disappear over a long enough period of time. These experiments strengthened earlier reports that the so-called 'slow mode' of

diffusion^{79,80} is due to removable aggregates,^{81,82,83} rather than to any fundamental equilibrium nature of the polyelectrolyte solutions.

Figure 7. Dissolution of PSS in pure water and water with NaCl. Light scattering and refractometer monitoring results. (Adapted from ref. 77)



Aggregation

At low angles and high dilution, scattering within the Rayleigh-Debye approximation increases as the square of the scatterer's mass. Hence, TDSLS is exquisitely sensitive to aggregation, oligomerization, micro-crystallization, micro-gelation, and other processes where polymer mass increases in time.

An example of the aggregation of a fluoropolymer in DMSO is shown in figure 8, expressed as I/Kc vs. t . The signature suggests diffusion controlled aggregation of chains

into larger and larger structures, which then attain a maximum value. These aggregates are themselves only metastable, as the solutions precipitates after several days.

Heterogeneous Time Dependent Light Scattering (HTDSLS)

Traditionally, the presence a population of large colloid scatterers amidst a population of weakly scattering polymers would render it impossible to make useful light scattering measurements. The idea of HTDSLS is to make the solution flow through a small scattering volume (around 10 nanoliters) so that the passage of large particles produces recognizable peaks amidst the polymer scattering background. With intensity sampling fast enough to recognize these peaks, both the scattering background due to pure polymer can be recovered, at the same time that the number density of large scatterers is determined. This has utility in situations where large scatterers are an integral part of a polymer solution; e.g. bacteria in a fermentation reactor that produce or hydrolyze biopolymers such as polysaccharides or proteins, or the formation of microgels or microcrystals in a polymerization reactor. Other applications include cases where solutions are so contaminated by large particles they would normally be unmeasurable.

Figure 8. Aggregation kinetics of a fluoropolymer (Moyses and Reed, unpublished)

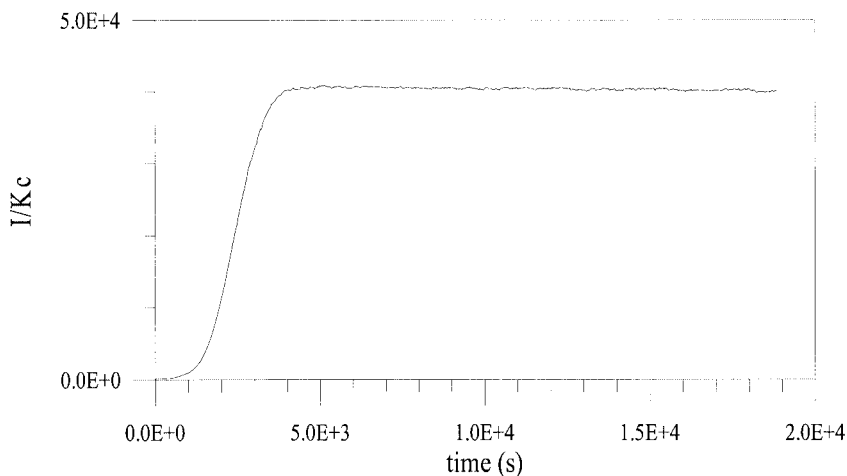
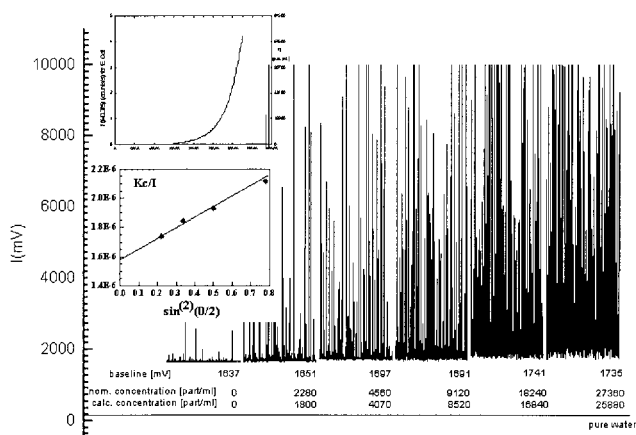


Fig. 9 shows an example of HTDSLS data, adapted from Schimanowski et al.,⁸⁴ in which a 0.1 mg/ml solution of PVP (650 Kg/mole) co-exists with a population of growing E.

Coli bacteria at 38⁰C. The PVP and E. Coli do not interact. The main portion of the data show the spikes due to E. Coli, and how the density of the spikes increases in time as the number density of bacteria increases. Despite the increase in E. Coli, the baseline scattering, which is due to the PVP, is easily recovered. The insets to the figure show the simultaneously obtained determination of Kc/I (yielding $\langle S^2 \rangle$ and M_w if A_2 is known), and the density of bacteria.

Figure 9. Co-existing polymers (PVP) and growing bacterial population (E.Coli). Spike density increases with bacterial growth. Insets show number density of bacteria and Kc/I for the polymer. (Adapted from ref. 84)



Automated methods for batch characterization

The automatic dilution used in ACOMP lends itself naturally to automated batch characterization when a sample is mixed in a continuous (or stepped) gradient with another sample solution, keeping the same detector train used in ACOMP. This yields a high resolution, continuous record of how light scattering and viscosity change as a function of a given solute; e.g. polymer, salt, or surfactant concentration. This significantly expands the scope of experimental investigation of simple and complex

polymer solutions, for which, traditionally, individual concentration samples would be manually prepared and measured.

Automated Zimm plot/intrinsic viscosity determination

Ref. 24 detailed the use of continuous dilution to produce a complete light scattering and viscosity characterization of water soluble polymers. Figure 10 shows the Zimm plot data for PVP in water. The inset shows the raw scattering intensity. A maximum value is reached, followed by a decline. This is due to the third virial coefficient A_3 .

Effect of changing ionic strength on polyelectrolyte conformations, interactions and hydrodynamics

It is well known that polyelectrolytes are sensitive to the ionic strength of the medium they are in. An extensive theoretical and experimental literature exists on how conformations, persistence lengths (PL), excluded volume, and hydrodynamics depend on electrostatic effects, whose magnitude, in turn, depends on ionic strength.^{85,86,87,88,89}

Recently, experiments were performed in which the concentration of polyelectrolyte was held fixed, and the ionic strength was increased continuously.⁹⁰ Figure 11 shows raw data on LS and viscosity vs. [NaCl] for sodium hyaluronate (HA). As expected, the light scattering intensity increases as salt increases, since the large, electrostatic contribution to excluded volume, and hence A_2 , decreases. At the same time, the contraction of the polyelectrolyte dimensions with increased screening decreases the hydrodynamic volume, and hence the polyelectrolyte's reduced viscosity.

The inset to the figure shows the viscosity as a function of [NaCl] for HA, xanthan and PSS, which immediately reveals the relative stiffness of these polymers. The xanthan is stiffest, with an intrinsic PL over 100nm. It quickly loses its electrostatically enhanced PL at low [NaCl] and its intrinsic stiffness allows no further contraction as [NaCl] increases. HA has intermediate flexibility, an intrinsic PL of 10nm, and it is seen that it contracts over the whole range of [NaCl], beginning to flatten out at the highest values. PSS has an intrinsic PL of about 1nm, and the viscosity continues to drop unabatedly over the whole range of [NaCl].

Figure 10. Automated Zimm plot determination for PVP.

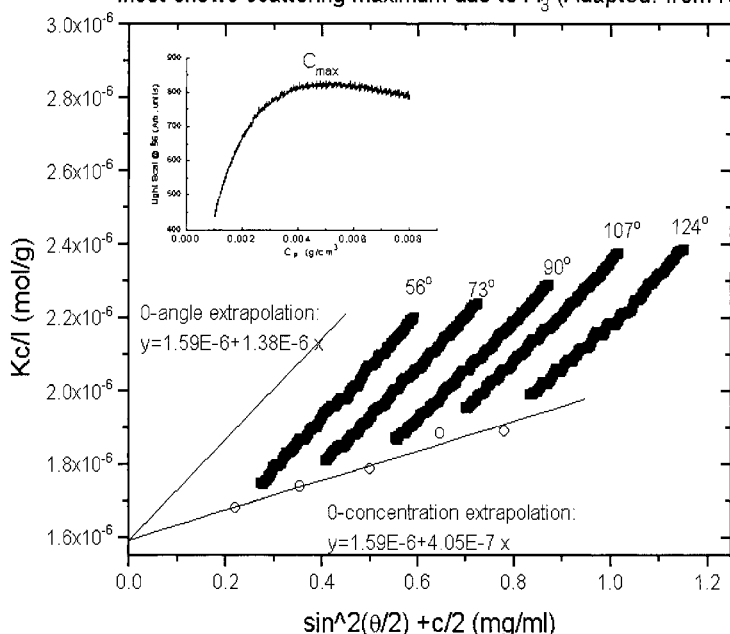
Inset shows scattering maximum due to A_3 (Adapted. from ref. 24)

Fig. 12 shows data on the electroviscous effect for polyelectrolytes.^{91,92,93} In this effect, as the polyelectrolyte solution is diluted with low ionic strength aqueous solvent there is a maximum value of η_r at a low polyelectrolyte concentration, after which further dilution leads to a decrease in η_r . The effect is usually attributed to the fact that because the counterions of the polyelectrolyte contribute to solution ionic strength, as dilution with a fixed ionic strength solvent proceeds, the net solution ionic strength decreases, leading to an expansion of the polyelectrolyte coils with a concomitant increase of both intrinsic viscosity and the interchain hydrodynamic interactions.^{93,94} Other areas where automated batch characterization is useful include multi-component systems, where complex interactions are expected. Any parameterized curves in the phase diagram can be programmed into the method. Currently, we are using the method to determine the phase

diagram, and the nature of aggregates formed between surfactant micelles and neutral and charged polymers.

Figure 11. Light scattering and viscometer response of a linear polyelectrolyte to increasing ionic strength. (Adapted from ref. 90)

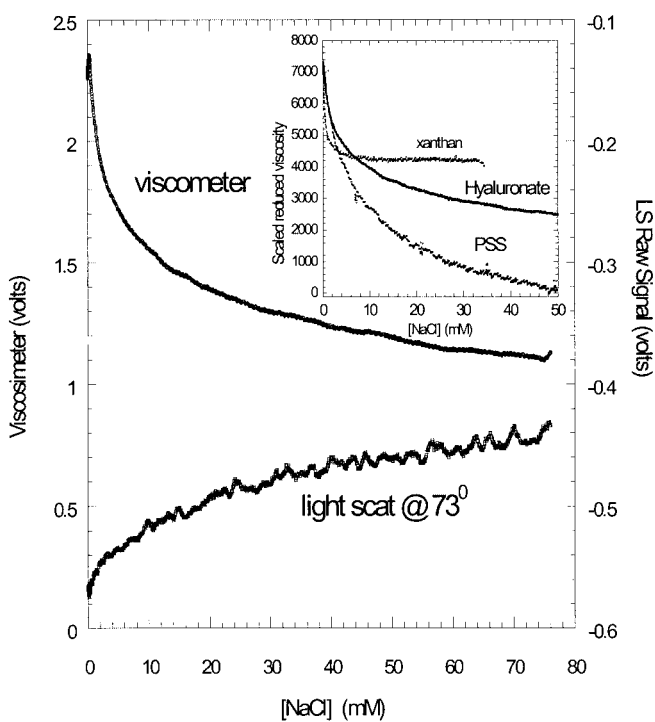
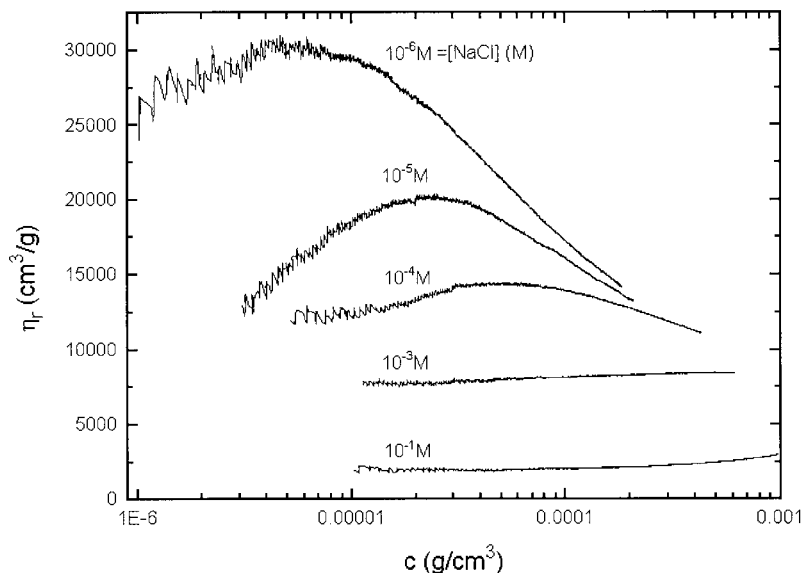


Figure 12. Electroviscous effect for hyaluronic acid (Strelitzki and Reed, unpublished)



Acknowledgments

I am grateful to many colleagues over the past few years who have participated in this work. These include Alan Parker, David Norwood, Corinne Vinches, Roland Strelitzki, Ruth Schimanowski, Fabio Florenzano, Ricardo Michel, Jean-Luc Brousseau, Stephan Moyses, Bruno Grassl, Joana Ganter, Erica Bayly, Gina Sorci, Alina Alb, Huceste and Ahmet Giz, and Florence Chauvin. Support from the U.S. National Science Foundation grant 9877206, Louisiana Board of Regents, Elf Atochem, Totalfina, Brookhaven Instruments Corp., Firmenich, and Int'l. Specialty Products is acknowledged.

¹ H. Holthoff, S.U. Egelhaaf, M. Borkovec, P. Schurtenberger, H. Sticher, *Langmuir*, 12, 5541-5549, 1996

² S.U. Egelhaaf, P. Schurtenberger, *Rev. Sci. Instrum.*, 67, 2, 540-545, 1996

³ L.S. Wright, A. Chowdhury, P. Russo, *Rev. Sci. Instrum.*, 67, 10, 3645-3648, 1996

⁴ E. Lai, J.H. Van zanten, *Biophys. J.*, 80, 2, 864-873, 2001

⁵ C. LeBon, T. Nicolai, D. Durand, *Macromolecules*, 32, 19, 6120-6127, 1999

⁶ R.M. Murphy, M.M. Pallitto, *J. Struct. Biol.*, 130, 2, 109-122, 2000

⁷ S. He, P.G. Arscott, V.A. Bloomfield, *Biopolymers*, 53, 4, 329-341, 2000

⁸ B. Barham, K. Fossier, G. Voge, D. Waldow, A. Halasa, *Macromolecules*, 34, 3, 514-521, 2001

- ⁹ A.J. O'Connor, T. A. Hatton, A. Bose, *Langmuir*, 13, 26, 6931-6940, 1997
- ¹⁰ S. Bernocco, S. Ferri, A. Profumo, C. Cuniberti, M. Rocco, *Biophys. J.*, 79, 561-583, 2000
- ¹¹ T. Norisuye, M. Shibayama, S. Nomura, *Polymer*, 39, 13, 2769-2775, 1998
- ¹² R. Bansil, L. Guandong, P. Falus, *Physica A: Stat. and Theor. Phys.*, 231, 3, 346-358, 1996
- ¹³ J. Kojima, Y. Nakayama, M. Takenaka, T. Hashimoto, *Rev. Sci. Inst.*, 66, 8, 4066-4072, 1995
- ¹⁴ H. Takeshita, T. Kanaya, K. Nishida, K. Kaji, *Macromolecules*, 32, 23, 7815-1819, 1999
- ¹⁵ R. Kita, T. Kaku, K. Kubota, T. Dobashi, *Phys. Lett. A*, 259, 4, 302-307, 1999
- ¹⁶ G.D. Merfeld, D.R. Paul, *Polymer*, 41, 2, 649-661, 2000
- ¹⁷ F. Mallamace, N. Micali, S.H. Chen, *Physica A: Stat. Theor. Phys.*, 235, 2, 170-185, 1997
- ¹⁸ R.S. Stein, J. Cronauer, H.G. Zachmann, *J. Molec. Struct.*, 383, 3, 19-22, 1996
- ¹⁹ M. Okamoto, T. Inoue, *Polymer*, 36, 14, 2739-2744, 1995
- ²⁰ A. Niu, C. Li, Y. Zhao, J. He, Y. Yang, C. Wu, *Macromolecules*, 34, 3, 460-464, 2001
- ²¹ B.H. Zimm, *J. Chem. Phys.*, 16, 12, 1093-1114, 1948
- ²² H.C. van de Hulst, *Light Scattering by Small Particles*, Wiley, N.Y., 1957
- ²³ M. Kerker, *The Scattering of Light and Other Electromagnetic Radiation*, Academic Press, N.Y. 1969
- ²⁴ R. Strelitzki, W.F. Reed, *J. App. Polym. Sci.*, 73, 2359-2368, 1999
- ²⁵ W.F. Reed, *Strategies for Size Exclusion Chromatography*, ACS ser. 635; Potschka, M., Dubin, P., Eds.; ACS: Wash. D.C., 1996; pp 7-34
- ²⁶ D.P. Norwood, W.F. Reed, *Int. J. Polym. Ana. and Char.*, 4, 2, 99-132, 1997
- ²⁷ P.J. Flory, *J. Am. Chem. Soc.*, 61, 3334-3340, 1939
- ²⁸ S.E. Bresler, E.N. Kazbekov and V.N. Shadrin, *Makromole. Chem.*, 175, 2875-2880, 1974
- ²⁹ J. Shen, Y. Tian, *Makromole. Chem. Rapid Comm.*, 8, 615-620, 1987
- ³⁰ D.G.H. Ballard, P.W. van Lienden, *Makromole. Chem.*, 154, 177-190, 1972
- ³¹ C. Jones, J.A. Brown, *Adv. in Instrumentation*. 38, Part 1. Proc. of ISA Int. Conf., p. 705, 1983
- ³² R.L. Grob, D.J. Skahan, K. Dix, K. Nielsen, *Process Control & Quality*, 2, 3, 225-35, 1992
- ³³ D.J. Ehntholt, R.F. Taylor, E.V. Misco, *ISA Trans.*, 32, 2, 183-8, 1993
- ³⁴ R.F. Storey, A.B. Donnalley, T.L. Maggio, *Macromolecules*, 31, 5, 1523-1526, 1998
- ³⁵ J. Mijovic, S. Andjelic, J.M. Kenny, *Polym. Adv. Technol.*, 7, 1, 1-16, 1996
- ³⁶ C. Gwosdz, M.S. Francis, A. Bickel, *Proc. Control Qual.*, 4, 1, 31-35, 1992
- ³⁷ M. Scott, *Control & Instrumentation*, 23, 3, 40-43, 1991
- ³⁸ R. Reshadat, S.T. Balke, *App. Spectroscopy*, 53, 10, 1309-1311, 1999
- ³⁹ P. Dallin, *Process Cont. and Qual.*, 9, 4, 167-172, 1997
- ⁴⁰ D.J.T. Hill, L.Y. Shao, P.J. Pomery, A.K. Whittaker, *Polymer*, 42, 11, 4791-4802, 2001
- ⁴¹ A. Penlidis, J.F. MacGregor, A.E. Hamielec, *Proc. of Amer. Control Conf.*, 2, 878-880, 1985
- ⁴² R.S. Saltzman, *I&CS*, 67, 2, 49-51, 1994
- ⁴³ Y.S. Kim, C. Sook, C. P. Sung, *J. Appl. Polym. Sci.*, 57, 3, 363-70, 1995
- ⁴⁴ H.J. Paik, N.H. Sung, *Polymer Eng. Sci.*, 34, 1025-1032, 1994
- ⁴⁵ A. Fuchs, N.H. Sung, *Polym. Mater. Sci. Eng.*, 71, 439-440, 1994
- ⁴⁶ M.G. Hansen, S. Vedula, *Polym. Process Eng.*, 97, 89-102, 1997
- ⁴⁷ J.M. Starita, C.L. Rohn, *Plast. Compd.*, 10, 2, 46-51, 1987
- ⁴⁸ O. Brand, J.M. English, S.A. Bidstrup, M.G. Allen, *Sensors and Actuators.*, 1, 121-124, 1997
- ⁴⁹ S. Ponnuswamy, S.L. Shah, C. Kiparissides, *J. Appl. Polym. Sci.*, 32, 1, 3239-53, 1986
- ⁵⁰ I.N. Kotchetov, D.C. Neckers, *J. Imaging Sci. & Tech.*, 37, 2, 156-163, 1993
- ⁵¹ W.F. Reed, L. Guterman, P. Tundo, J.H. Fendler, *J. Am. Chem. Soc.*, 106, 1897-1907, 1984
- ⁵² W. F. Reed, *Macromolecules*, 18, 2402-2409, 1985
- ⁵³ F.H. Florenzano, R. Strelitzki, W.F. Reed, *Macromolecules*, 1998, 31, 7226-7238
- ⁵⁴ A. Giz, H.C. Giz H.C., A. Alb, J.L. Brousseau, W.F. Reed, *Macromolecules*, 34, 1180-1191, 2001
- ⁵⁵ N.A. Dotson, R. Galvan, R.L. Laurence, M. Tirrel, *Polymerization Process Modeling*, VCH Pub. N.Y. 1996
- ⁵⁶ T. Ishige, A.E. Hamielec, *J. App. Polym. Sci.*, 17, 1479 -1506, 1973
- ⁵⁷ J.P. Riggs, F. Rodriguez, *J. Polym. Sci. A-1*, 5, 3151 -3181, 1967
- ⁵⁸ W.F. Reed, *Macromolecules*, 33, 7165-7172, 2000
- ⁵⁹ W. Burchard, *Static and Dynamic Light Scattering from Branched Polymers and Biopolymers*, in *Advances in Polymer Sci.*, 48, Springer Verlag, Berlin, 1983
- ⁶⁰ J.F. Douglas, J. Roovers, K.F. Freed, *Macromolecules*, 23, 4168-80, 1990
- ⁶¹ C.E. Ioan, T. Aberle and W. Burchard, *Macromolecules*, 33, 5730-39, 2000

- ⁶² A. Giz, H. Giz, J.L. Brousseau, A. Alb and W.F. Reed, *J. Appl. Polym. Sci.*, in press, 2001
- ⁶³ F. Chauvin, A. Alb, D. Bertin, P. Tordo, W.F. Reed, *Macromolecules*, submitted
- ⁶⁴ B. Grassl, W.F. Reed, *Am Inst. Chem. Eng. J.*, submitted
- ⁶⁵ B. Grassl, A. Alb, W.F. Reed, *Makromole. Chem. Phys.*, in press, 2001
- ⁶⁶ C.A. Thomas, *J. Amer. Chem. Soc.*, 78, 1861-1866, 1956
- ⁶⁷ W.F. Reed, *J. Chem. Phys.*, 103, 7576-7584, 1995
- ⁶⁸ C.E. Reed, W.F. Reed, *J. Chemical Physics*, 91, 7193-7199, 1989.
- ⁶⁹ W.F. Reed, C.E. Reed, L. Byers, *Biopolymers*, 30, 1073-1082, 1990
- ⁷⁰ S. Ghosh, I. Kobal, D. Zanette, W. F. Reed, *Macromolecules.*, 26, 17, 4685-4693, 1993
- ⁷¹ S. Ghosh, W.F. Reed, *Biopolymers*, 5, 435-450, 1995
- ⁷² L.H. Catalani, A.M. Rabello, F.H. Florenzano, M.J. Politi, W.F. Reed, *Int. J. Polym. Char. Anal.*, 3, 2, 231-247, 1997
- ⁷³ J.L. Ganter, J. Sabi, J., W.F. Reed, *Biopolymers*, in press, 2001
- ⁷⁴ D.J. Buckley, M. Berger, *J. Polym. Sci.*, 56, 175-179, 1962
- ⁷⁵ F. Brochard, P.G. De Gennes, *Physicochem. Hydrodynam.*, 4, 313-319, 1983
- ⁷⁶ I. Devotta, V. Premnath, M.V. Badiger, P.R. Rajamohanan, S. Ganapathy, R.A. Mashelkar, *Macromolecules*, 27, 532-539, 1994
- ⁷⁷ R.C. Michel, W.F. Reed, *Biopolymers*, 53, 19-39, 2000
- ⁷⁸ A. Parker, F. Vigouroux, W.F. Reed, *Am. Inst. Chem. Eng. Journal*, 46, 7, 1290-1299, 2000
- ⁷⁹ S.C. Lin, W.I. Lee, J.M. Schurr, *Biopolymers*, 17, 1041-1064, 1978
- ⁸⁰ M. Drifford, J.P. Dalbiez, *Biopolymers*, 24, 1501-1514, 1984
- ⁸¹ S. Ghosh, R.M. Peitzsch, W.F. Reed, *Biopolymers*, 32, 1105-1122, 1992
- ⁸² X. Li, W.F. Reed, *J. Chem. Phys.*, 94, 4568-4580, 1991
- ⁸³ R.G. Smits, M.E. Kuil, M. Mandel, *Macromolecules*, 27, 5599-5608, 1994
- ⁸⁴ R. Schimanowski, R. Strelitzki, D.A. Mullin, W. F. Reed, *Macromolecules*, 32, 21, 7055-7063, 1999
- ⁸⁵ T. Odijk, *J. Polym. Sci. Phys. Ed.*, 10, 9444-9451, 1977
- ⁸⁶ M. Fixman, J. Skolnick, *Macromolecules*, 11, 8638-8644, 1978
- ⁸⁷ W.F. Reed, S. Ghosh, G. Medjehadi, J. Francois, *Macromolecules*, 24, 6189-6202, 1991
- ⁸⁸ S. Förster, M. Schmidt, *Adv. Polym. Sci.*, 120, 51-133, 1995
- ⁸⁹ C.E. Reed, W.F. Reed, *J. Chem. Phys.*, 94, 8479-8486, 1991
- ⁹⁰ Bayly, E., Brousseau, J.L., Reed, W.F., *Int. J. Polym. Char. and Anal.*, in press, 2001
- ⁹¹ S. Basu, *Nature*, 168, 341-343, 1951
- ⁹² W.F. Reed, *J. Chem. Phys.*, 101, 3, 2515-2521, 1994
- ⁹³ R.M. Fuoss, V.P. Strauss, *J. Polym. Sci.*, 3, 602-609, 1948
- ⁹⁴ M. Rinaudo, M. Milas, M. Jouon, R. Borsali, *Polymer*, 34, 17, 3710-3718, 1993